

LA-UR- *09-00184*

Approved for public release;
distribution is unlimited.

<i>Title:</i>	in situ PEM Fuel Cell Water Measurements
<i>Author(s):</i>	Rod L. Borup Mukundan Rangachary John R Davey Jacob Spendelow Muhammad Arif David Jacobson Daniel Hussey
<i>Submitted to:</i>	2008 Fuel Cell Seminar & Exposition issue of ECS Transactions



Los Alamos National Laboratory, an affirmative action/equal opportunity employer, is operated by the University of California for the U.S. Department of Energy under contract W-7405-ENG-36. By acceptance of this article, the publisher recognizes that the U.S. Government retains a nonexclusive, royalty-free license to publish or reproduce the published form of this contribution, or to allow others to do so, for U.S. Government purposes. Los Alamos National Laboratory requests that the publisher identify this article as work performed under the auspices of the U.S. Department of Energy. Los Alamos National Laboratory strongly supports academic freedom and a researcher's right to publish; as an institution, however, the Laboratory does not endorse the viewpoint of a publication or guarantee its technical correctness.

In Situ PEM Fuel Cell Water Measurements

Rod L. Borup^a, Rangachary Mukundan^a, John R. Davey^a, Jacob Spendelow^a, Daniel S. Hussey^b, David L. Jacobson^b, Muhammad Arif^b

^a Los Alamos National Laboratory, MS D429, MPA-11, Los Alamos, NM 87545

^b National Institute of Standards and Technology (NIST), Center for Neutron Research, 100 Bureau Drive, MS 8461, Gaithersburg, MD 20899

Efficient PEM (Polymer Electrolyte Membrane) fuel cell performance requires effective water management. To achieve a deeper understanding of water transport and performance issues associated with water management, we have conducted in situ water examinations to help understand the effects of components and operations. High Frequency Resistance (HFR), AC Impedance and Neutron imaging were used to measure water content in operating fuel cells, with various conditions, including current density, relative humidity, inlet flows, flow orientation and variable Gas Diffusion Layer (GDL) properties.

High resolution neutron radiography was used to image fuel cells during a variety of conditions. The effect of specific operating conditions, including flow direction (co-flow or counter-flow) was examined. Counter-flow operation was found to result in higher water content than co-flow operation, which correlates to lower membrane resistivity.

A variety of cells were used to quantify the membrane water in situ during exposure to saturated gases, during fuel cell operation, and during hydrogen pump operation. The quantitative results show lower membrane water content than previous results suggested.

Introduction

Efficient PEM fuel cell performance requires effective water management. The combinations of materials used, their durability, and the operating conditions under which fuel cells run, make efficient water management within a practical fuel cell system a primary challenge in developing commercially viable systems. Automotive polymer electrolyte membrane (PEM) fuel cells will likely operate with inlet gas streams at less than saturated conditions and will experience numerous and varied power transients. Both of these factors will affect the water dynamics of the Membrane Electrode Assembly (MEA) as well as other fuel cell components. This hydration state of the MEA and GDLs before and between these power transients will affect the fuel cell system performance. It is therefore important to understand the water dynamics of the PEM fuel cell MEA and GDLs in response to power transients.

To gain a greater understanding of water transport within PEM fuel cells, we made *in situ* measurements of water in operating fuel cells to examine the material and operational effects on water transport. These *in situ* measurements included imaging of water via

neutron imaging, measurement of protonic conductivity of the membrane (thus indicating the amount of water in the membrane), correlating AC Impedance to the other in situ water measurements, and X-Ray tomography measurements of GDL materials.

Experimental

The fuel cell hardware used for testing includes standard single serpentine flow field 50 cm² hardware from Fuel Cell Technologies and 2.25 cm² cell specially designed for high resolution neutron imaging. Most MEAs used were Gore™ Primea® MEA Series 57 with 18 μ m thick GORE-SELECT® membranes with carbon-supported 0.2 mg Pt/cm² on the cathode and 0.1 mg Pt cm² on the anode (GORE-SELECT, PRIMEA and GORE are trademarks of W. L . Gore & Associates, Inc). The GDLs used were SGL Carbon's carbon paper GDLs with specified polytetrafluoroethylene (PTFE) loadings in the substrate and microporous layer (MPL).

Other MEAs used to quantify the membrane water content by neutron imaging were prepared by directly applying Pt black to the membrane in protonic form. To make the Pt-black electrodes, an ink of HISPEC 1000 Pt-black catalyst, 5% solution of 1100EW Nafion® from Solution Technology, and water, that when dried is 10 wt% Nafion, is mixed briefly with a sonicator. A pre-measured quantity of the ink was painted on the masked "active area" of a dry protonated Nafion® membrane, and held flat on a heated 70C vacuum table. Several coats were required to achieve the desired loading of 6 mg Pt/cm². Thick Nafion® membranes (~ 500 micron) were provided by Ion Power.

Neutron Imaging

Neutron imaging was performed at the NIST Center for Neutron Research (NCNR) on thermal beam tube 2.(1) HRR measurements were made every second during the neutron imaging. Neutron image analysis was performed using the IDL programming language and a dry reference image as described by Hickner et al.(2)

Results and Discussion

Distribution of Water

Fig. 1 shows a typical water thickness image for a 2.25 cm² active area cell for different operating modes. Fig. 1a shows co-flow operation (anode and cathode inlets at the same end of the flowfield), while Fig. 1b shows counter flow operation (inlets at opposite ends of the flowfield). Operating conditions were 80 °C, with anode stoichiometry = 1.2, cathode stoichiometry = 2, 100% RH anode and cathode feeds, and current density = 1.4 A/cm². The cathode is on top, while the

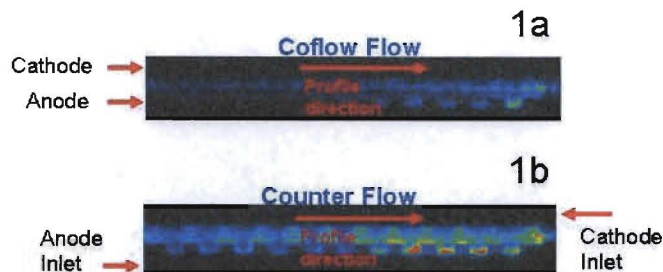


Fig. 1. Water thickness image calculated from high resolution neutron radiograph. (a) **Co-flow** : $I = 1.41$ A/cm²; $V = 0.095$ V; HFR = 0.10 Ohm cm². (b) **Counter Flow** : $I = 1.49$ A/cm²; $V = 0.27$ V; HFR = 0.064 Ohm cm²

anode is on the bottom. Significantly more water is observable with counter flow operation, even though the operating conditions were essentially identical.

Fig. 2 shows the water thickness in the MEA (membrane plus catalyst layer) down the profile of the flowfield for (a) co-flow and (b) counter flow. Substantially more water is present in the membrane in the counter flow operation; approximately 3 – 4x the quantity of water. The additional water in the membrane agrees qualitatively with the HFR measurements of $HFR = 0.10$ (a) and 0.064 $\text{Ohm}\cdot\text{cm}^2$ (b) for the two operational cases showing that counter flow operation leads to additional membrane water, and better membrane conductivity.

Fig. 3 shows the water thickness in the MEA plus GDL for the same conditions as Fig. 2. The co-flow case is shown in Fig. 3a with counter flow shown in Fig. 3b. Similar to Fig. 2, more water is present for operation with counter flow as compared with co-flow. However, in contrast is the large variation in water thickness for counter flow, which coincides with the flowfield land and channels. Water that is generated at the MEA during fuel cell operation must be transported through either the anode or cathode GDLs to be removed via the flowfields. If the water is generated under a land, it must first be transported to a part of the GDL that is under a channel in order to escape into the flow field. Therefore, the amount of water in parts of the MEA and the GDLs that are under lands is generally higher than the amount of water under channels.

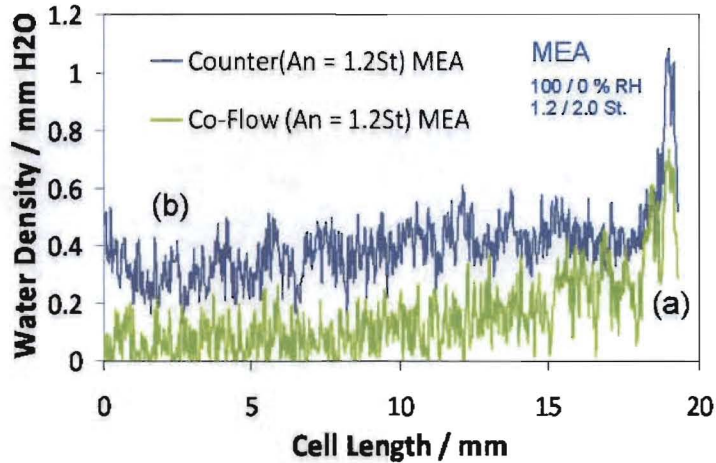


Fig. 2. Average water density down the length of the flowfield profile in the MEA (membrane and catalyst layer) for (a) co-flow and (b) counter flow. Cell operating conditions: 80°C , anode stoichiometry = 1.2, cathode stoichiometry = 2, 100% RH anode feed, 100% RH cathode feed, current density = $1.2 \text{ A}/\text{cm}^2$.

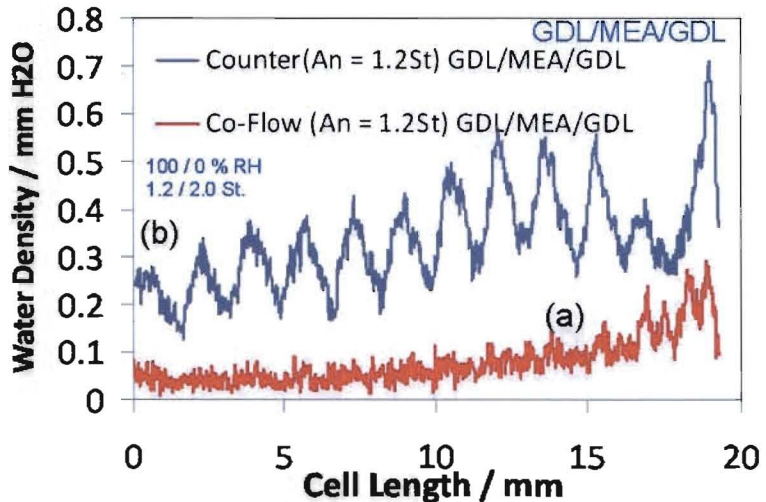


Fig. 3. Average water density down the length of the flowfield profile in the MEA plus GDL for (a) co-flow and (b) counter flow. Cell operating conditions same as Fig. 2.

the anode or cathode GDLs to be removed via the flowfields. If the water is generated under a land, it must first be transported to a part of the GDL that is under a channel in order to escape into the flow field. Therefore, the amount of water in parts of the MEA and the GDLs that are under lands is generally higher than the amount of water under channels.

Water Quantification

It has previously been observed(3,4) that the amount of water in the membrane in a high resolution neutron imaging cross-section lacks good agreement with the prior experimental results of Zawodzinski et al.(5). Part of this discrepancy is possibly due to the detector resolution and detector spread function.(4) An example of this discrepancy is shown in Fig. 4 for a N117 MEA operated at 100% RH. Note that Lambda has been defined as $\lambda = 1$ $\text{H}_2\text{O}/\text{SO}_3\text{H}$, and λ hereafter. λ for each current density is also shown. Note that the measured λ are below the normally cited literature value of 14 for Nafion® exposed to 100% water saturated vapor.(5) The λ of the sample only reaches 10 equilibrated at 100% RH. As the operating current of the cell was increased, the membrane water content did not increase for this sample. However there have been questions about the quantification of the membrane water because of the thickness of the MEA samples.

To eliminate the issue with the detector resolution (~ 25 micron), we used MEAs with thick membranes. Two different sets of experiments were done, one with a ‘sandwich’ of three 7 mil membranes and one 2 mil Nafion® membrane for a total membrane thickness of 584 microns. The other used a special cast single membrane of ~ 500 micron in thickness. These MEAs were then equilibrated with humidified gases with the water thickness measured via neutron imaging.

Fig. 5 shows the water profile across the MEA as a function of various equilibrating conditions. For the cases in which the membrane was exposed to only water in vapor state,

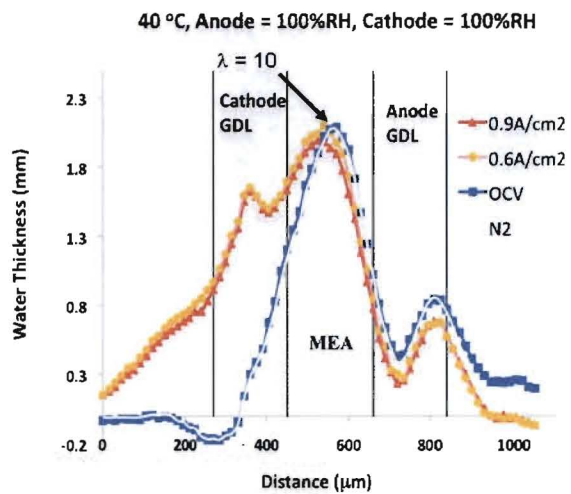


Fig. 4. Water density profile of an operating fuel cell with a Nafion® 117 membrane..

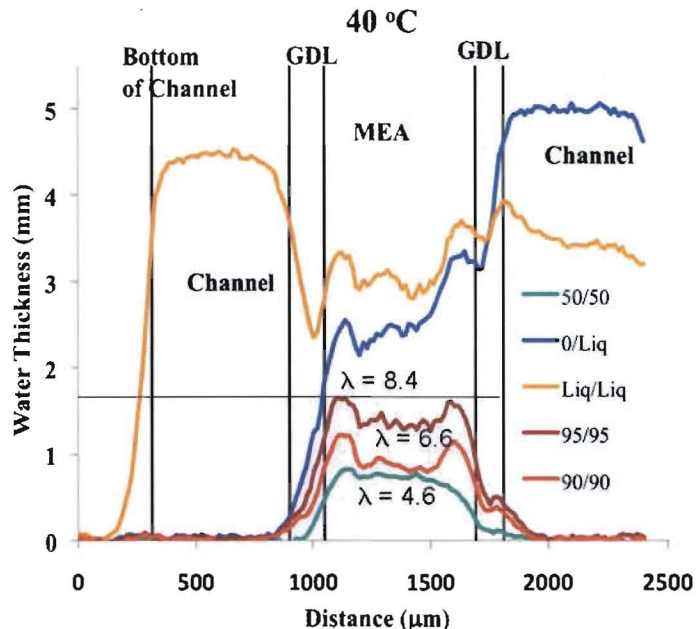


Fig. 5. Water density profile of a membrane ‘sandwich’ of 3x 7 mil plus 2 mil Nafion® membranes equilibrated with various levels of humidified gases.

the λ did not go above 8.4 (for 95% inlet RH). Upon exposure to water in the liquid state, λ reached 19.4. Unfortunately, the results, as observed in Fig. 5, are not ideal as the membrane 'sandwich' has interfaces between the individual membrane layers which affect the membrane water content. There appear to be hydophilic interfaces in the sample, especially at the membrane/catalyst interface, while more hydrophobic regions are found elsewhere in the sample--complicating understanding of the membrane water content.

To remove the issues with the membrane interfaces, a single thick (50 micron) membrane was used. The membrane water content for this cell was measured at open circuit voltage (OCV), with operating fuel cell current, and in hydrogen pump mode (operating current without water production). The water density profile of the 500 micron thick membrane is shown in Fig. 6 for (a) OCV, (b) 0.1 Amp/cm² and (c) 0.2 Amp/cm². For the case of no current flow and no water production at OCV (a), the measured λ is only 8.3. As the cell is operated at low current densities of 0.1 and 0.2 A/cm², the membrane λ increases as a function of the current density to 10.5 and 11.5.

Fig. 7 shows the MEA operating in hydrogen pump mode, which resulted in water profiles similar to those shown in Fig. 6. In this case, a potentiostat is used to drive current across the MEA, with the anode side exposed to hydrogen, and the cathode exposed to nitrogen with both gases fully humidified. This operation is similar to fuel cell mode, with the exception that no water is produced in the cell. The membrane water content increased as a function of pumping current density, however, for all cases

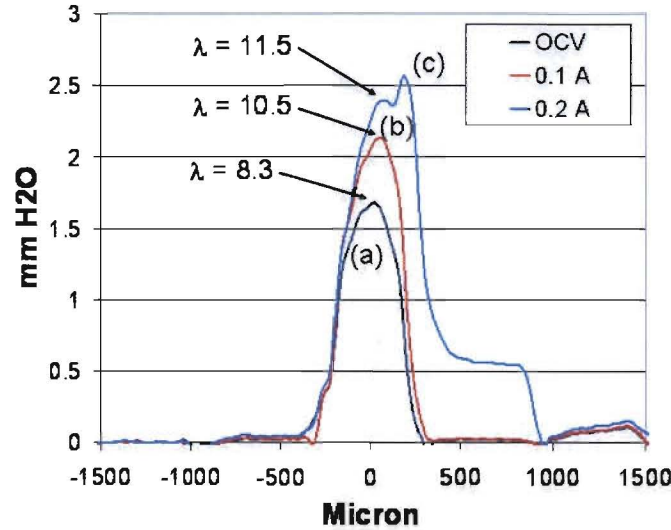


Fig. 6. Water density profile of an operating fuel cell with a 20 mil thick Nafion® membrane. Operating conditions were 100% inlet RH (anode and cathode) and 40C.

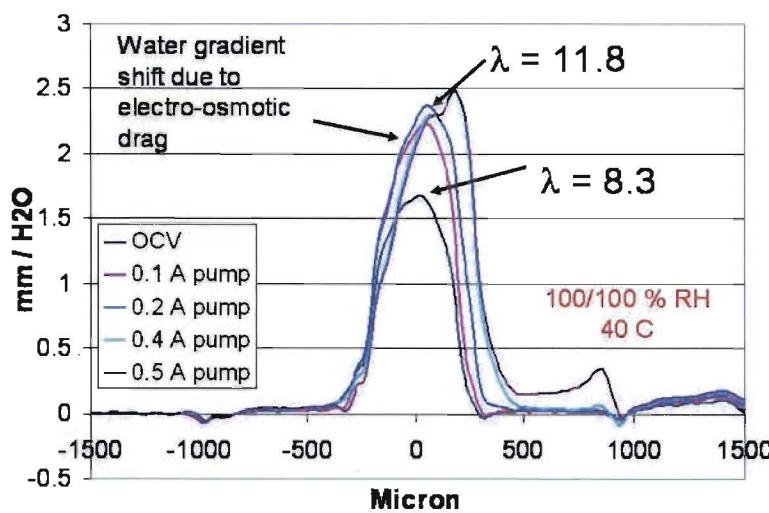


Fig. 7. Water density profile of an MEA operating in hydrogen pump mode with a 20 mil thick Nafion® membrane. Operating conditions were 100% inlet RH (anode and cathode) and 40C.

remains below the expected value of 14. The highest measured λ was 11.8 at a current density of 0.5 A/cm^2 . The water profiles also show a shift in location in the cell to the cathode which is consistent with electro-osmotic drag moving the water profile towards the cathode.

Conclusions

High resolution neutron radiography allows water content in individual cell components to be quantified and compared under different operating conditions. The direct measurement of the effect of operating conditions on water distribution, especially when combined with cell performance data, provides information that is valuable in understanding the factors that limit performance, as well as in developing strategies for improving performance.

Flow direction significantly impacts total water content, as well as water distribution, within an operating fuel cell. Co-flow operation results in highly non-uniform water distribution, in which water content increases down the length of the cell from inlets to outlets. In contrast, counter-flow operation produces more uniform water distribution, with higher total water content.

Quantification of the water within the membrane under exposure to different humidified gases, during fuel cell operation and in hydrogen pump mode suggests that the membrane water content is lower than prior experiments suggest.

Acknowledgments

This work was supported by the Office of Hydrogen Fuel Cells and Infrastructure Technologies at the U.S. Department of Energy-Energy Efficiency and Renewable Energy. This work was also supported by the U.S. Department of Commerce, the NIST Ionizing Radiation Division, the Director's Office of NIST, the NIST Center for Neutron Research, and the Department of Energy through interagency agreement no. DE-AI01-01EE50660.

We also acknowledge Steve Grot of Ion Power for preparing thick (20 mil/500 micron) Nafion® membranes for use in neutron imaging.

References

1. Rangachary Mukundan, Yu Seung Kim, Tommy Rockward, John R. Davey, Bryan S. Pivoar, Daniel S. Hussey, David L. Jacobson, Muhammad Arif, and Rodney L. Borup, *ECS Transactions*, 2007; v.11, no.1, p.543-552.
2. M. A. Hickner, N. P. Siegel, K. S. Chen, D. N. McBrayer, D. S. Hussey, D. L. Jacobson, and M. Arif, *J. Electrochem. Soc.*, Vol. 153, No. 5, A902 (2006).
3. Weber, A. Z.; Hickner, M. A., *Electrochimica Acta* (2008), 53(26), 7668-7674.
4. Borup, R. L., U.S. DOE Hydrogen Program Merit Review, Arlington Va, May 2008.
5. T. A. Zawodzinski, Jr., C. Derouin, S. Radzinski, R. J. Sherman, V. T. Smith, T. E. Springer, and S. Gottesfeld, *J. Electrochem. Soc.*, Vol. 140, No. 4, April 1993.

Certain trade names and company products are mentioned in the text or identified in an illustration in order to adequately specify the experimental procedure and equipment used. In no case does such identification imply recommendation or endorsement by the National Institute of Standards and Technology, nor does it imply that the products are necessarily the best available for the purpose.